Monthly Notices of the ROYAL ASTRONOMICAL SOCIETY

MNRAS 00, L1 (2022) https://doi.org/10.1093/mnrasl/slac094

Diurnal variation of the surface temperature of Mars with the Emirates Mars Mission: a comparison with Curiosity and Perseverance rover measurements

Dimitra Atri,★ Nour Abdelmoneim, Dattaraj B. Dhuri and Mathilde Simoni

Center for Space Science, New York University Abu Dhabi, PO Box 129188, Saadiyat Island, Abu Dhabi, UAE

Accepted 2022 August 11

ABSTRACT

For the first time, the Emirates Mars Infrared Spectrometer (EMIRS) instrument on board the Emirates Mars Mission (EMM) 'Hope', is providing us with the temperature measurements of Mars at all local times covering most of the planet. As a result, it is now possible to compare surface temperature measurements made from orbit with those from the surface by rovers during the same time period. We use data of diurnal temperature variation from the Rover Environmental Monitoring Station (REMS) suite on board the Mars Science Laboratory (MSL) 'Curiosity' rover, and the Mars Environmental Dynamics Analyzer (MEDA) suite on board the Mars 2020 'Perseverance' rover, between June and August 2021 and compare them with EMIRS observations and estimates of the Mars Climate Database (MCD) model. We show that although the overall trend of temperature variation is in excellent agreement across missions, EMIRS measurements are systematically lower at night compared to Mars 2020. The lower spatial resolution of EMIRS compared to the rovers and consequently lower average thermal inertia of the observed regions in this particular case primarily contributed to this discrepancy, among other factors. We discuss the implications of these results in improving our understanding of the Martian climate which would lead to better modeling of local weather prediction, useful for future robotic and crewed missions.

Key words: space vehicles – planets and satellites: surfaces.

1 INTRODUCTION

The transformation of Mars from a warm, wet planet with potentially habitable conditions to a cold and dry planet that we see today is an active area of research by space agencies around the globe (Bhardwaj 2014; Vago et al. 2015; Zurbuchen 2017; Amiri et al. 2022). It is not only important to investigate this in order to understand Mars, but for enabling us to better understand the evolution of Earth and other planets in the Solar system and beyond (Sagan & Mullen 1972; Jakosky 2021). A number of atmospheric and surface processes occurring on Mars at present provide us with clues to this long-term transformation of the planet. Studying the diurnal and seasonal variability of the surface temperature of Mars is of prime importance because of its key role in governing a number of surface, shallow subsurface, and lower atmospheric processes of the planet and its influence on weather, climate, and the eventual escape of volatiles from the atmosphere (Petrosyan et al. 2011).

Surface temperature measurements have been made in the past from orbiters, such as the Thermal Emission Spectrometer (TES) instrument on board the Mars Global Surveyor (MGS; Christensen et al. 2001), the Planetary Fourier Spectrometer (PFS) instrument (Formisano et al. 2005) on board Mars Express (MEX), the Thermal InfraRed channel in honour of professor Vassilii Ivanovich Moroz (TIRVIM), a part of the Atmospheric Chemistry Suite (ACS) onboard the ExoMars Trace Gas Orbiter (TGO; Korablev et al. 2018), Mars Reconnaissance Orbiter/Compact Reconnaissance Imaging Spectrometer for Mars (MRO/CRISM; He et al. 2022), Mars Odyssey/Thermal Emission Imaging System (MO/THEMIS; Edwards et al. 2018). Such measurements have also been made by landers and rovers, such as the Viking landers 1 and 2 (Hess et al. 1977), Mars Exploration Rovers (MER), Spirit and Opportunity (Spanovich et al. 2006; Mason & Smith 2021), Rover Environmental Monitoring Station (REMS) on board the Mars Science Laboratory (MSL) 'Curiosity' (Gómez-Elvira et al. 2012; Martínez et al. 2021), Mars Environmental Dynamics Analyzer (MEDA) on board the Mars 2020 'Perseverance' rover (Rodriguez-Manfredi et al. 2021; Martinez et al. 2022), and the Heat flow and Physical Properties Package (HP3) for the InSight mission (Spohn et al. 2018; Piqueux et al. 2021). Depending on the orbit, satellite measurements have the advantage of geographical coverage, they suffer from a lack of local time coverage. On the other hand, rovers provide measurements at all local times, but the measurements are confined geographically. The Emirates Mars Mission (EMM) or 'Hope' aims to fill-in this gap in observations (Almatroushi et al. 2021).

One of the main goals of EMM is to provide a global view of Mars on diurnal and seasonal time-scales. EMM's unique orbit enables it to observe the spatial distribution of surface and near-surface temperature for most of the planet at all local times (Almatroushi et al. 2021; Edwards et al. 2021;Amiri et al. 2022). It also enables measurements of diurnal temperature variations over full Martian day with near-complete coverage of the entire planet. Since we are able to observe diurnal temperature variations at most locations on

★ E-mail: da99@nyu.edu

Mars, it opens an opportunity to directly compare observations from the orbit and from the surface of Mars.

In this letter, we report diurnal temperature variation for the most of the planet measured by EMM from orbit and compare it with surface measurements made by MSL (Gómez-Elvira et al. 2012) and Mars 2020 (Rodriguez-Manfredi et al. 2021) rovers over the same time period. We describe a number of factors which could lead to these differences in measurements and propose solutions. We also compare these measurements with the Mars Climate Database (MCD; Millour et al. 2018) and discuss implications for improved modelling of Martian weather and climate.

2 SPACECRAFT MEASUREMENTS

2.1 Orbiter: EMIRS/EMM

The Emirates Mars Infrared Spectrometer (EMIRS) instrument (Edwards et al. 2021) on board EMM is a Fourier Transform Infra Red (FTIR) spectrometer observing in 6–100 μm wavelength range. It is designed to provide measurements of the lower atmosphere and surface of Mars by conducting thermal infrared observations of the disc. It provides diurnal measurements over the entire globe on sub-seasonal time scales. EMM's orbital period is $\sim$ 55 h with a periapsis of 20 000 km and an apoapsis of 43 000 km. It takes $\sim$20 observations per orbit or $\sim$60 per week with one observation taking 29 min at periapsis and 11 min at apoapsis. It takes 4 orbits or less than 10 d to obtain the global coverage at all local times. The resolution ranges between 100 to 300 km pixel^{-1} (diameter) with up to 70° emission angle. Level 2 data products (L2) contain calibrated radiance and brightness temperature. Level 3 products (L3), used in this study, are derived from L2 and have corrected surface temperatures among other quantities. Surface temperatures (L3) are obtained using a three-step process (Edwards et al. 2021): first the atmospheric temperatures are retrieved from the 15 μm CO_2 band, then dust optical depth and water-ice aerosol optical depths are fit, and finally the water vapour column depth is fit. This retrieval process is iterated until convergence, and quality control metrics are used to ensure the quality of final retrieved products. A comparison of L2 and L3 measurements is shown in the Appendix Fig. A1.

The orbiter was inserted in the Martian orbit on 2021 February 9 (MY 36, L_s = 0.6) providing 9 sols of EMIRS observations for the month from the insertion orbit. The orbiter was in transition orbit for the next couple of months, starting the science phase of the mission from 2021 May 23 (L_s = 48.7).

Fig. 1 shows the diurnal surface temperature variation over 30 sols for L_s = 65.8–78.9 (2021 July). The horizontal and vertical axes show latitude and longitude in degrees respectively. The surface temperature is colour-coded in units of Kelvin and the time shown is the Local True Solar Time (LTST). We constructed these maps by dividing the planet into 10° × 10° latitude/longitude bins. Appendix Fig. B1 shows the number of samples in each spatial bin. We then obtained a temperature value for each bin by averaging the surface temperature measurements during each of the 3-h time intervals. In both the polar regions, data above 80° is scarce. For the northern polar region, the data are very limited between 14:00 - 20:00 h and for the southern polar region, data is very limited between 02:00 - 14:00 h. One can easily notice the large-scale variation in surface temperature across the planet in a given time slot, and also global changes in temperature over the course of the sol. Temperatures in the Northern hemisphere are systematically higher corresponding to the summer season. As expected, the daily temperature variability is most noticeable in the

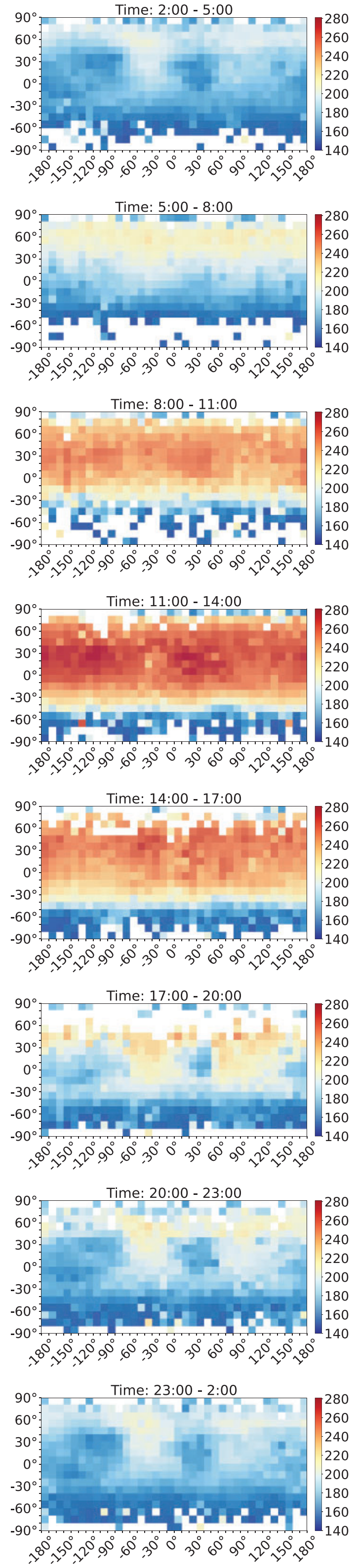

Figure 1. Global surface temperature map based on EMIRS/EMM observations of 30 sols L_s = 65.8–78.9 (2021 July).

northern mid-latitudes. Global temperature maps for other months are available in the Appendix Figs B2–B4.

2.2 Surface rover: REMS/MSL

The REMS (Sebastián et al. 2010) instrument on board MSL provides meteorological measurements at the rover's location in Gale crater on diurnal and seasonal scales (Gómez-Elvira et al. 2012). Gale crater, the operating site of MSL, is located in the Aeolis Quadrangle at the edge of the dichotomy boundary. It has a diameter of 154 km, is 4 km below datum at the landing site and features Mount Sharp, which is 1.5 km above datum. Ground and air temperature measurements are available over periods overlapping with EMM observations. Measurements are taken by two orthogonally placed booms – Boom 1 hosts the Air Temperature Sensor (ATS) and the Ground Temperature Sensor (GTS), and Boom 2 hosts another ATS. GTS, which is mounted on Boom 1, measures the IR brightness temperature of the surface with three thermopiles. REMS measures the ground brightness temperature in the 150–300 K range with an accuracy of 1 K and a resolution of 2 K (Martínez et al. 2017). The air temperature is also measured by both the booms with the same accuracy and resolution.

The initial data was obtained from MODRDR (Models RDR) files containing the REMS instrument's highest level data product for every sol. The ground brightness temperature as a function of LTST were extracted from sols 3018 to 3224, a total of 207 sols for MY 36, L_s = 1.1 - 92.5. An initial cleaning of the data set revealed an average 1959 null values per sol, ranging from 845 to 10246 rows. This resulted in an average of 23 180 readings taken at a rate of 1 Hz for each sol. The data points were first grouped by month (to be consistent with EMM SDC) and subsequently by hour intervals during the day. For each hour interval, the mean, minimum and maximum values as well as the standard error were calculated and plotted on the following graphs.

2.3 Surface rover: MEDA/Mars 2020

The MEDA suit of sensors on board the Mars 2020 rover provides continuous meteorological data from the Jezero crater, including surface temperature measurements (Rodriguez-Manfredi et al. 2021). Jezero crater has a 49 km diameter and is located in the Isidis basin (1500 km) on the dichotomy boundary. The near-surface atmospheric circulation is influenced by the local and regional topography (Pla-García et al. 2020; Newman et al. 2021, 2022). The Thermal InfraRed Sensor (TIRS; Sebastián et al. 2021) is a part of MEDA and is an Infrared (IR) radiometer measuring the brightness temperature of the surface. In particular, IR5 provides the ground temperature, measuring in the 8–14 μm band, with a dynamic range of 173–293 K, an accuracy of $\pm$ 0.75 K, and a resolution of 0.08 K.

The ground brightness temperature as a function of LTST were extracted from TIRS between sols 15 to 188, corresponding to MY 36, L_s = 13–92. While data was available starting 2021 February 18, TIRS was not deployed for the first few sols, therefore, we started our analysis from March 6. We found that data points were missing for 7 sols: sols 23, 24, 25, 26, and 27 in March, sol 97 in May, and sol 183 in August, leading to a total of 167 sols included in the analysis. Time intervals corresponding to sol 168 (14:00–16:30), sol 177 (14:00–15:00), and sols 159, 161, 163, 167, 169, and 171 (03:00–04–00) were then removed from the analysis due to calibration activities which resulted in values that are not representative Martínez (2022). This initial cleaning revealed an average of 45 518 data points per sol, ranging from 4207 to 59 135 rows and including 0 null values. The data points were first grouped by month (to keep it consistent with EMM SDC) and subsequently by hour intervals during the day. For each hour interval, the mean, minimum and maximum values as well as the standard error were calculated and plotted on the following graphs.

2.4 The Mars climate data base MCD

The MCD provides averaged data on the main meteorological variables such as pressure, temperature, atmospheric density, and winds (Millour et al. 2018). It is a derived from Laboratoire de Météorologie Dynamique LMD–GCM Wolfgang & Lopez (2015), a Global Climate Model (GCM) of Mars, which includes a water cycle model, a chemistry model, a thermosphere model, and an ionospheric model. It provides day-to-day variability of main meteorological variables and is widely used in the Mars community. In addition to the output from GCM, it provides high-resolution environmental data, year-to-year variability, dust content variations, seasonal and diurnal cycles of key meteorological variables. We obtain the diurnal variability of surface temperatures from MCD at the sites of the Curiosity and Perseverance rovers at Gale and Jezero crater respectively, in order to compare with the temperature observations from EMIRS. Appendix Fig. C1 shows locations of the Curiosity and Perseverance rovers.

3 COMPARISON OF MEASUREMENTS

3.1 EMM, MSL, and MCD

Fig. 2 shows the hourly surface temperature measurement comparisons from REMS and EMIRS at the MSL rover site over (Gale crater) ~ 30 sols for L_s = 65.8–78.9 (2021 July) and 79.3–92.5 (2021 August), respectively. We sample the EMIRS temperature measurements from $2^\circ \times 2^\circ$, $3^\circ \times 3^\circ$, $5^\circ \times 5^\circ$, $7^\circ \times 7^\circ$, $10^\circ \times 10^\circ$, $15^\circ \times 15^\circ$, and $20^\circ \times 20^\circ$ region centred at the MSL location. Wherever EMIRS observations are available, the peak temperatures show a good match, while the lowest temperatures recorded by REMS are slightly higher. Fig. 3 shows the corresponding average diurnal temperatures, along with the temperatures predicted by the MCD model at the MSL rover site. The average diurnal variation pattern is identical in both EMIRS and REMS temperature measurements and consistent with the MCD model predictions. The average daily temperatures start rising at 05 h and reach a peak value of approximately 250 K at around 13 h in all cases. The EMIRS temperature measurements fall more rapidly after the peak and, in general, the afternoon, evening, and night time temperatures are markedly lower compared to measurements by REMS and the MCD model. The temperatures recorded by REMS are generally consistent with the MCD model predictions for the morning and the afternoon. However, they are systematically higher than the MCD model predictions for the night time. The average lowest temperatures vary significantly and are 170 K, 180 K, and 190 K for EMIRS, MCD, and REMS, respectively.

3.2 EMM, Mars 2020, and MCD

Fig. 2 shows hourly surface temperature measurement comparisons from MEDA and EMIRS at the Perseverance rover site (Jezero crater) over ~ 30 sols for L_s = 65.8–78.9 (2021 July) and 79.3–92.5 (2021 August), respectively. Compared to EMIRS, the Perseverance temperature measurements show low maximum to minimum daily temperature variability, and this variability is particularly low for sols 10–25 in July. Fig. 4 shows the corresponding average diurnal

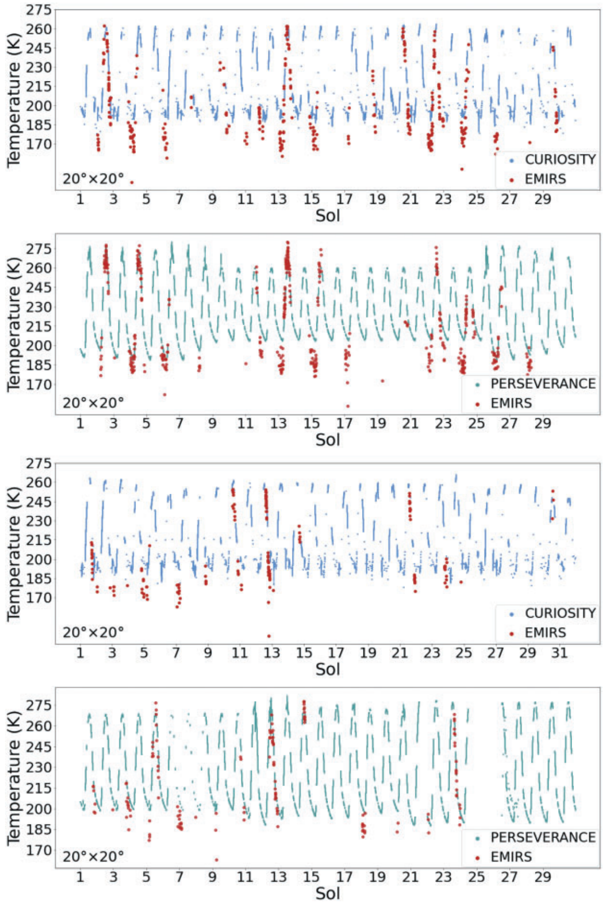

Figure 2. Comparison of hourly surface temperatures between EMIRS, REMS/MSL, and MEDA/Mars 2020 over ∼ 30 sols for L_s = 65.8 -78.9 [2021 July, sols 3164–3194 (REMS/MSL) and sols 128–158 (MEDA/Mars 2020), *top two panels*] and for L_s = 79.3–92.5 [2021 August, sols 3194–3224 (REMS/MSL) and sols 158–188 (MEDA/Mars 2020), *bottom two panels*]. Each point corresponds to a single observation and gaps indicate missing observations.

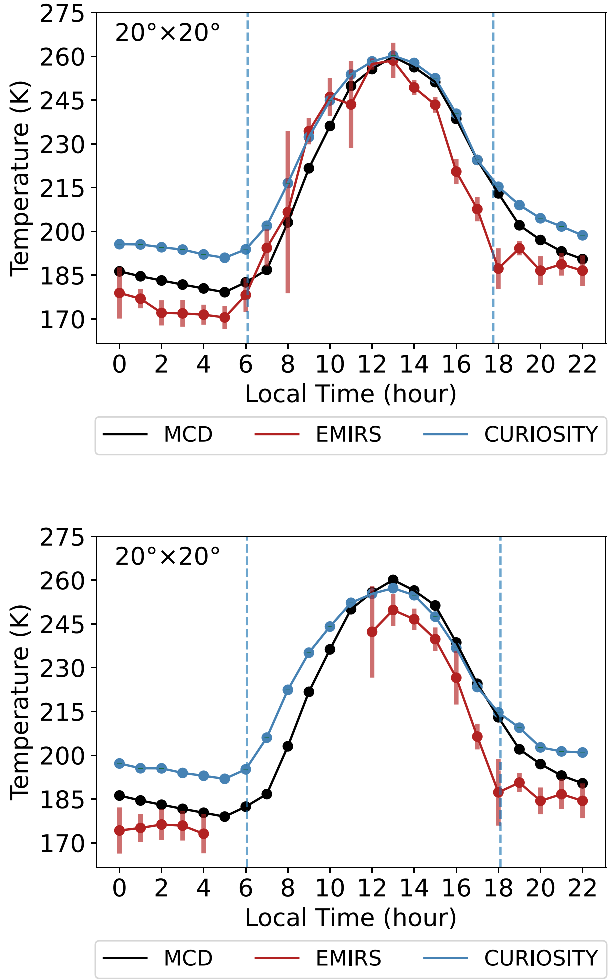

Figure 3. A comparison of average diurnal temperature variation measured by EMIRS/EMM and REMS/MSL with the model prediction from MCD. *Top panel*: Over ∼ 30 sols for L_s = 65.8–78.9 (2021 July, sols 3164–3194). *Bottom panel*: Over ∼ 30 sols for L_s = 79.3–92.5 (2021 August, sols 3194–3224). The error bars indicate 3 σ standard errors. Local dawn and dusk are marked by vertical lines.

temperature variation, along with the temperatures predicted by the MCD model at the Perseverance rover site. The average diurnal variation pattern is identical in both the EMIRS and the Curiosity temperature measurements and consistent with the MCD model predictions. The average daily temperatures start rising from 04 h and reach a peak value at around 13 h in all cases. The peak temperature values recorded by EMIRS and Perseverance are approximately equal and are ∼ 10 K lower than the MCD model peak temperature of ∼ 270 K. The MCD model predicts afternoon temperatures that are systematically higher by ∼10 K compared to EMIRS, with temperatures obtained by Perseverance falling in between. The night-time temperatures recorded by EMIRS remain lower compared to the MCD model, whereas the Perseverance temperature measurements are slightly higher. The lowest temperatures recorded by EMIRS, MCD, and Perseverance are ∼ 180 K, ∼ 190 K, and ∼ 200 K, respectively. Appendix Figs C2–C5 show hourly EMIRS surface temperature comparisons with Curiosity and Perseverance observations for other months as well as smaller field of views (FOV) of EMIRS about the rover locations. Appendix Figs D2–D5 show corresponding comparisons for average diurnal temperatures.

4 CONCLUSION AND DISCUSSION

EMM observations, for the first time have enabled us to study the surface temperatures at all local times for most locations on Mars. This has enabled us to compare EMM/EMIRS observations taken from the orbit at overlapping times with surface rovers MSL and Mars 2020. We find that the overall trend in daily temperature variability is consistent between different missions and also with MCD estimates. Hourly temperature variability of EMIRS is in good agreement with MSL. However, EMIRS measurements are systematically lower, especially at night-times at lowest temperatures. There could be several reasons leading to this discrepancy in measurements. One potential issue with this analysis is the vast difference between the FOV of EMIRS (as discussed earlier) and rovers. Although measurements from rovers are sensitive to variability arising from both small-scale local and large-scale regional features, EMIRS is sensitive to only large-scale regional features. Within the FOV of EMIRS, a number of geological units with varying thermal inertia and surface roughness could exist (see Appendix Figs E1–E3). Different thermal inertia of rocks, dust, and sand would result in uneven rate of change of temperature, influencing the diurnal temperature

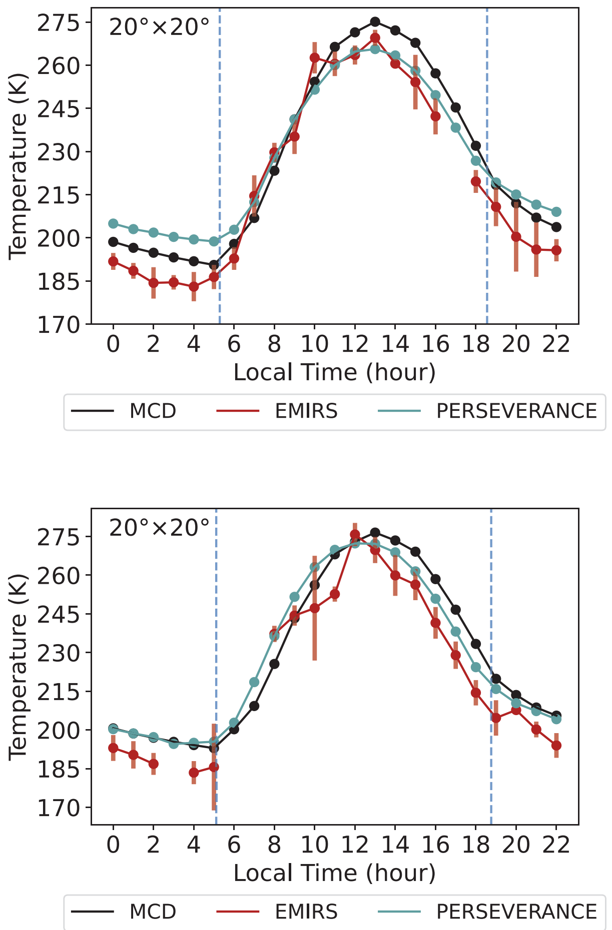

Figure 4. A comparison of average diurnal temperature variation measured by EMIRS/EMM and MEDA/Mars 2020 with the model prediction from MCD. *Top panel*: Over ∼ 30 sols for L_s = 65.8–78.9 (2021 July, sols 128–158). *Bottom panel*: Over ∼ 30 sols for L_s = 79.3–92.5 (2021 August, sols 158–188). The error bars indicate 3 σ standard errors. Local dawn and dusk are marked by vertical lines.

variation. Also, brightness temperature obtained from observations is highly sensitive to rock abundance, especially at night (Wolfe et al. 2022). Preliminary work by Wolfe et al. (2022) found that EMIRS observations are sensitive to rock abundance, especially near the equator and mid-latitude regions. The surface scattering and emission also depends on the roughness of the surface, which in turn would lead to differences in estimated values of surface temperature. The seemingly odd kinks in EMIRS averaged data (Figs 3 and 4) are an artefact of the non-uniform spatial sampling from the larger FOV, and go away at smaller FOV as seen in figures D4 and D5 in the appendix. The corresponding number of observations are lower and error bars are larger, and hence these apparent peaks are not significant for the diurnal temperature variation trends discussed.

EMIRS observations with smaller grid size are taken in a similar thermal environment as rovers averaged over a period of time. Being an instrument on board an orbiter, having a low spatial resolution is a limitation of EMIRS. With more observations made by the orbiter, we hope to create a better picture of the thermal environment of Mars, which will also enable better comparison with rover measurements. More work needs to be done in order to disentangle the influence of regional versus local features, between different rock units and other factors such as surface roughness which might influence the estimates of surface temperature, and this analysis is an important first step in that direction. Additionally, estimates from climate models too vary significantly, for example, up to 10 K difference in surface temperature was seen across nine different models in the Jezero crater region (Newman et al. 2021). With this work of comparing observations made from the orbit with those from the surface, we hope to better constrain models leading to advancements in weather and climate modeling, especially model-to-model differences. We plan to compare seasonal changes observed between different missions though one Mars-year, which is also the duration of EMM's primary mission. This effort will also assist with improved planning of future robotic missions (Fonseca, Zorzano & Martín-Torres 2019) as well as crewed missions to the planet (Drake, Hoffman & Beaty 2010).

ACKNOWLEDGEMENTS

This work was supported by the New York University Abu Dhabi (NYUAD) Institute Research Grant G1502 and the ASPIRE Award for Research Excellence (AARE) Grant S1560 by the Advanced Technology Research Council (ATRC). This work utilized the High Performance Computing (HPC) resources of NYUAD. We thank Prof. K. R. Sreenivasan for his constant encouragement and support for the project.

DATA AVAILABILITY

EMM data was obtained from the EMM Science Data Center (SDC), and MSL and Mars 2020 data from NASA's Planetary Data System (PDS), both are open access repositories.

REFERENCES

Almatroushi H. et al., 2021, Space Sci. Rev., 217, 1
Amiri H. et al., 2022, Space Sci. Rev., 218, 1
Bhardwaj A., 2014, 40th COSPAR Scientific Assembly, 40, C3
Christensen P. R. et al., 2001, J. Geophys. Res.: Planets, 106, 23823
Drake B. G., Hoffman S. J., Beaty D. W., 2010, IEEE Aerospace Conference. p. 1
Edwards C. S. et al., 2018, J. Geophys. Res.: Planets, 123, 1307
Edwards C. S. et al., 2021, Space Sci. Rev., 217, 1
Fonseca R. M., Zorzano M.-P., Martín-Torres J., 2019, Earth Space Sci., 6, 1440
Formisano V. et al., 2005, Planet. Space Sci., 53, 963
Gómez-Elvira J. et al., 2012, Space Sci. Rev., 170, 583
He L., Arvidson R., O'Sullivan J., Morris R., Condus T., Hughes M., Powell K., 2022, J. Geophys. Res.: Planets, e2021JE007092
Hess S., Henry R., Leovy C. B., Ryan J., Tillman J. E., 1977, J. Geophys. Res., 82, 4559
Jakosky B. M., 2021, Annu. Rev. Earth Planet. Sci., 49, 71
Korablev O. et al., 2018, Space Sci. Rev., 214, 1
Martínez G. et al., 2017, Space Sci. Rev., 212, 295
Martínez G. et al., 2021, J. Geophys. Res.: Planets, 126, e2020JE006804
Martinez G. et al., 2022, LPI Contributions, 2678, 2024
Mason E. L., Smith M. D., 2021, Icarus, 360, 114350
Millour E., Forget F., Spiga A., Vals M., Zakharov V., Montabone L., 2018, in From Mars Express to ExoMars, 27-28 February 2018. Madrid, Spain
Newman C. et al., 2021, Space Sci. Rev., 217, 1
Newman C. E. et al., 2022, Sci. Adv., 8, eabn3783
Petrosyan A. et al., 2011, Rev. Geophys., 49
Piqueux S. et al., 2021, J. Geophys. Res.: Planets, 126, e2021JE006859
Pla-García J. et al., 2020, Space Sci. Rev., 216, 1
Rodriguez-Manfredi J. A. et al., 2021, Space Sci. Rev., 217, 1
Sagan C., Mullen G., 1972, Science, 177, 52

Sebastián E., Armiens C., Gómez-Elvira J., Zorzano M. P., Martinez-Frias J., Esteban B., Ramos M., 2010, Sensors, 10, 9211
Sebastián E., Martínez G., Ramos M., Pérez-Grande I., Sobrado J., Manfredi J. A. R., 2021, Acta Astronaut., 182, 144
Spanovich N., Smith M., Smith P., Wolff M., Christensen P., Squyres S., 2006, Icarus, 180, 314
Spohn T. et al., 2018, Space Sci. Rev., 214, 1
Vago J. et al., 2015, Sol. Syst. Res., 49, 518
Wolfe C. A., Edwards C. S., Smith M. D., Christensen P. R., Smith N. M., Badri K., Anwar S., 2022, in LPI Contributions, Vol. 2678, LPI Contributions. p. 2804
Wolfgang A., Lopez E., 2015, ApJ, 806
Zurbuchen T. H., 2017, Presentation to the National Academies, 28

SUPPORTING INFORMATION

Supplementary data are available at *MNRAS* online.

Appendix A. Emirs L2 and L3 Surface Temperature Comparison.
Appendix B. Global Surface Temperature Measurements.
Appendix C. Hourly Temperature Comparisons.
Appendix D. Diurnal Coverage as a Function of Spatial Grid Size for Selecting Emirs Observations About the Location of the Curiosity and Perseverance Rovers' Landing Sites.
Appendix E. Thermal inertia comparisons.

Please note: Oxford University Press is not responsible for the content or functionality of any supporting materials supplied by the authors. Any queries (other than missing material) should be directed to the corresponding author for the article.

This paper has been typeset from a TEX/LATEX file prepared by the author.